Evidence for structural transition in hairy-rod poly[9,9-bis(2-ethylhexyl)fluorene] under high pressure conditions

M. Knaapila,[1,2,*] R. Stepanyan,[3] D. Haase,[2] S. Carlson,[2] M. Torkkeli,[4] Y. Cerenius,[2] U. Scherf,[5] and S. Guha[6]
[1]*Physics Department, Institute for Energy Technology, NO-2027 Kjeller, Norway*
[2]*MAX-lab, Lund University, SE-22100 Lund, Sweden*
[3]*Materials Science Centre, DSM Research, NL-6160 MD Geleen, The Netherlands*
[4]*Department of Physics, FI-00014 University of Helsinki, Finland*
[5]*Fachbereich Chemie, Bergische Universität Wuppertal, D-42097 Wuppertal, Germany*
[6]*Department of Physics and Astronomy, University of Missouri, Columbia, Missouri 65211, USA*
(Received 8 September 2010; published 22 November 2010)

We report on an x-ray scattering experiment of bulk poly[9,9-bis(2-ethylhexyl)fluorene] under quasihydrostatic pressure from 1 to 11 GPa at room temperature. The scattering pattern of high molecular weight (HMW) polyfluorene (>10 kg/mol) undergoes significant changes between 2 and 4 GPa in the bulk phase. The 110 reflection of the hexagonal unit cell disappears, indicating a change in equatorial intermolecular order. The intensity of the 00 21 reflection drops, with a sudden move toward higher scattering angles. Beyond these pressures, the diminished 00 21 reflection tends to return toward lower angles. These changes may be interpreted as a transition from crystalline hexagonal to glassy nematic phase (perceiving order only in one direction). This transition may be rationalized by density arguments and the underlying theory of phase behavior of hairy-rod polyfluorene. Also the possible alteration of the 21-helical main chain toward more planar main chain conformation is discussed. The scattering of low molecular weight polyfluorene (<10 kg/mol), which is glassy nematic in ambient pressure, is reminiscent with that of HMW polymer above 2–4 GPa.

DOI: 10.1103/PhysRevE.82.051803 PACS number(s): 36.20.−r, 62.50.−p, 64.60.Cn

I. INTRODUCTION

Phase behavior [1] is an ubiquitous topic in the materials science of hairy-rod polymers [2,3] such as π-conjugated polymers (CPs) [4]. Among these materials, polyfluorenes (PFs) [5,6] are particularly interesting as they represent not only a structural archetype [7] but also a key motif for polymer electronics [8].

Overwhelming majority of the structural studies of CPs has been carried out at ambient pressure. In particular, while the high pressure x-ray diffraction (XRD) of inorganic materials has been long at an advanced state [9], corresponding reports of CPs are almost nonexistent. A high pressure XRD study of poly(3-octylthiophene) (POT) of Mårdalen *et al.* [10] represents an exception. A high pressure XRD study of fluorene molecule [11] is also known.

Indirect structural information comes from the optical studies of compressed CPs and oligomers including poly(*p*-phenylene vinylene) [12], ladder-type poly(*p*-phenylene)s [13], *p*-hexaphenyl [14], and polydiacetylene crystals [15]. Prime examples of the optical studies of PFs at elevated pressure include studies of poly(9,9-di-*n*-octylfluorene) by Guha and co-workers [16,17] and studies of poly(9,9-di-*n*-octylfluorene-*alt*-benzothiadiazole) by Schmidtke *et al.* [18,19]

Poly[9,9-bis(2-ethylhexyl)fluorene] (PF2/6) has a complex solid-state structure consisting of a helical main chain [20–22] that organizes into hexagonal (Hex) and nematic (Nem) phases depending on the temperature and molecular weight [23]. Helicity of the main chain is found for branched (nonchiral, racemic, or chiral) side chains, besides the bis(2-ethylhexyl)-substituted PFs also for poly[9,9-bis((S)-2-methyloctyl)fluorene] [24] or poly[9,9-bis((S)-3,7-dimethyloctyl)fluorene] [25], but not in any of the more widely studied class of linear side-chain PF derivates [7]. The helical main chains organize into trimeric bundles with a hierarchic structure and cause effects such as multiple orientation of crystallites in biaxially aligned thin films [20]. PF2/6 was initially thought to form a 5/2 or 5/1 helix (i.e., 20/8 or 20/4 helix) [21], and this behavior was ascribed to a "soft pentagon" that is fundamentally incommensurate with the hexagonal symmetry. More recently, after a further refinement, a 21/4 helical form has been proposed [26,27]. Nonsymmetric branched side chains such as 2-ethylhexyl usually comprise a racemic mixture of both enantiomers and cannot crystallize as readily as linear side chains. This inherent disorder is likely the decisive factor at play whether the helicity is due to the side chains themselves or the packing frustration of chains represented by pentagons or heptagons.

Guha and co-workers [28,29] performed systematic high pressure photoluminescence (PL) and Raman scattering studies of PF2/6 both in bulk and in thin films. The authors reported that when the hydrostatic pressure exceeds 2 GPa, the PL of bulk PF2/6 undergoes a sudden and significant enhancement in the 2.1–2.6 eV emission. This contribution stems from aggregates (~2.4 eV) and from the keto defects (~2.3 eV). Although the fraction of defects is marginal at ambient pressure, their emission becomes enhanced supposedly because of enhanced intermolecular interactions with increasing pressure. The Raman peaks were found to harden with increasing pressure. The authors considered in particular a Raman peak at 1605 cm^{-1}, an intraring carbon-carbon

*Author to whom correspondence should be addressed. FAX: +47-6381-0920; matti.knaapila@ife.no

stretch mode. The asymmetry in line shape was analyzed in terms of the Breit-Wigner-Fano line shape equation $I(\omega)=I_0[(\omega-\omega_0)/q+\Gamma]^2/[(\omega-\omega_0)^2+\Gamma^2]$, where ω_0 is the discrete phonon frequency, Γ is the width of the resonant interference between the continuum and discrete scattering channels, and $1/q$ is an asymmetry parameter that depends on the electron-phonon interactions. The authors found that this peak shows increasing asymmetry (a drop of $1/q$) and broadening at 2–4, GPa, largely simultaneously with the changes in PL spectra, occurring in a stepwise fashion. The authors also indicated that the sudden changes in the relative intensities of PL emission resemble those expected for a crystalline–liquid-crystalline phase transition, the Hex-Nem transition in the terminology of Ref. [23].

The findings of Guha and co-workers encouraged us to perform wide-angle x-ray scattering (WAXS) experiments of PF2/6 at elevated pressures. The obtained data point to a morphological transition between 2 and 4 GPa. This transition thus coexists with the previously reported transition in PL and Raman scattering. In one scenario, the transition is akin to Hex-Nem phase transition, as also supported by theoretical considerations. In alternative scenario, the transition involves partial planarization of the helical main chain. Phenomenological arguments supporting this idea are provided, too.

II. THEORY

The hypothesis of PF2/6's pressure-induced phase transition [28] leads us to extending the theory of hairy-rod PF2/6. We first consider how elevated pressure would influence our previously presented picture of PF2/6 as a hairy-rod molecule with the Nem and Hex phases with a first-order phase transition [23]. In our previous work the pressure was always assumed constant (and normal atmospheric pressure).

For the first-order phase transition, the shift in the transition temperature as a function of pressure is described by the Clausius-Clapeyron relation [30]

$$\frac{dT^*}{dP}=\frac{V_N-V_H}{S_N-S_H}, \tag{1}$$

where T^* denotes the Nem-Hex transition temperature and V_i and S_i are the volume and entropy of the Nem ($i=N$) and Hex ($i=H$) phases.

An expression for the transition temperature T^* as a function of the molar mass and other parameters has been derived earlier [23]. In brief, this derivation is based on the free energies (per molecule) of the Nem and Hex phases as

$$F_N \approx k_B T \ln\frac{f}{e}+k_B T \ln\frac{4\pi}{\Omega_N}, \tag{2}$$

$$F_H \approx k_B T \ln\frac{4\pi}{\Omega_H}-k_B T\frac{\nu}{c\nu_0 l_K^2 l_u}, \tag{3}$$

where f is the volume fraction of the backbone, c is the number density of the molecules, ν and l_K are the volume of one side-chain bead and the Kuhn segment length of the side chain, and ν_0 and l_u are the volume and the length of the repeat unit of a hairy-rod molecule. In our previous publication [23] the "orientation angles" Ω_i were introduced as

$$\frac{\Omega_N}{\Omega_H}=\left(\frac{1+C_N t}{1+C_H t}\right)^{Ml_u/l_K^{HR}}, \tag{4}$$

where M is the number of repeat units per hairy-rod and l_K^{HR} is the Kuhn length of the molecule. The coefficients C_N and C_H represent the temperature dependence of the orientational ordering and $t=T-T_g$ is the reduced temperature with the temperature T and the glass transition temperature T_g.

Phase equilibrium between the two phases is achieved when the free energies [Eqs. (2) and (3)] are equal, which yields the reduced temperature

$$t^*=A\left(1-\frac{M_{n0}^*}{M_n}\right), \tag{5}$$

where A includes all the experimental parameters except the number averaged molecular weight M_n and $M_{n0}^* \approx [M_u l_K^2 l_u/\nu]\ln(e/f)$, which is M_n for the Hex-Nem transition at T_g. In Ref. [23] M_{n0}^* was calculated in dimensional units giving $M_{n0}^* \approx 10^4$ g/mol, a value well corresponding to the experimental data. The parameter $A \approx 90$ K was directly fitted to the experimental data. If $M_n < M_{n0}^*$, the polymer is denoted as low molecular weight (LMW) PF2/6, and if $M_n > M_{n0}^*$, it is denoted as high molecular weight (HMW) PF2/6.

We want next to shed some light on the transition temperature as a function of the applied pressure. Although Eqs. (2) and (3) are written for an incompressible material, they allow us to estimate the entropy jump at the transition point. Using $S=-(\partial F/\partial T)_V$ we find

$$S_N=-\frac{F_N}{T}+k_B T\frac{\partial \ln \Omega_N}{\partial T}, \tag{6}$$

$$S_H=-\frac{F_H}{T}+k_B T\frac{\partial \ln \Omega_H}{\partial T}, \tag{7}$$

where we have neglected the temperature dependence of all the other parameters except Ω's. Noticing that at the transition point $F_N=F_H$, we find for the entropy jump

$$(S_N-S_H)_{T=T^*} \sim k_B T\left.\frac{\partial \ln(\Omega_N/\Omega_H)}{\partial T}\right|_{T=T^*}, \tag{8}$$

and after insertion of Eq. (4),

$$(S_N-S_H)_{T=T^*} \sim k_B T^*\frac{Ml_u}{l_K^{HR}}(C_N-C_H). \tag{9}$$

Finally, using Eq. (1) we find

$$\frac{dT^*}{dP}=\frac{AM_{n0}^*}{RT^*}\left(\frac{1}{\rho_N}-\frac{1}{\rho_H}\right), \tag{10}$$

where ρ_i denotes the densities of phases at the transition point and R is the gas constant.

The very first observation we can make is that $dT^*/dP<0$ because, as follows from the experiment below, $\rho_N>\rho_H$. This corresponds to the potential decrease in transition

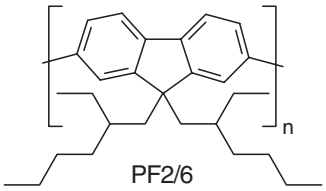

FIG. 1. Chemical structure of PF2/6 polymer.

temperature. It would be tempting to integrate Eq. (10) to reveal the $T^*(P)$ dependence in an explicit form. However, this would require at least the knowledge of the temperature and pressure dependence of the densities ρ_N and ρ_H. Yet we dare to estimate the order of magnitude of the T^* shift by assuming all the coefficients in Eq. (10) to be constant in temperature and pressure. The result is

$$T^{*2} = T^{*2}_{ref} - \frac{2AM^*_{n0}}{R\ln(e/f)}\left(\frac{1}{\rho_N} - \frac{1}{\rho_H}\right)(P - P_{ref}), \qquad (11)$$

where P_{ref} is the (normal atmospheric) reference pressure and T^*_{ref} is the transition temperature at the reference conditions.

The last expression can be rewritten in terms of pressures:

$$P^* = P_{ref} + \frac{R\ln(e/f)}{2AM_{n0}}\frac{\rho_N\rho_H}{\rho_N - \rho_H}(T^{*2}_{ref} - T^2), \qquad (12)$$

where T denotes the temperature at which the compression experiment is performed (here, room temperature) and P^* is the pressure when a Hex-Nem transition is expected. This expression and the description above are valid for nonglassy polymers.

III. EXPERIMENT

The synthesis of PF2/6 (Fig. 1) has been described elsewhere [31]. Three different PF2/6 samples were used with M_n and weight averaged molecular weight (M_w) as 3 and 5 kg/mol (denoted as 3/5-PF2/6), 29 and 68 kg/mol (29/68-PF2/6), and 39 and 58 kg/mol (39/58-PF2/6), respectively. HMW polymers were annealed at 180 °C for 10 min prior to use. This temperature is above their Hex-Nem transition (<160 °C) [23].

The WAXS measurements were performed using the high pressure x-ray scattering setup on the beamline I711 in MAX-lab in Lund [32]. The x-ray wavelength was $\lambda = 0.979$ Å. The beam was collimated with the slits of 0.55×0.55 mm^2 (vertical × horizontal).

Samples were loaded into a diamond-anvil cell (Diacell DXR-6 GM) following the procedure detailed in Ref. [33]. The sample chamber formed in this pressure cell was 100 μm high and 150–200 μm in diameter. Pressures up to 20 GPa are easily reached with this equipment. To minimize pressure gradients in the sample chamber, a methanol:ethanol (4:1) mixture was used as a quasihydrostatic pressure transmitting medium. The diamond-anvil cell was mounted on a motorized translation and rotation stage that was installed in the Mardtb Goniostat. The sample-to-detector distance was 27.7 cm, leading to the effective q range of 0.3–1.3 Å^{-1}. The scattering patterns were measured using a Marresearch SX-165 single charge-coupled device detector. The typical measurement time was 300 s. The sample alignment and pressure adjustment took about 30 min per pressure reading, which means that the pressure was increased in a stepwise manner by 1–2 GPa/h. LaB_6 (>98%, MaTecK) was used as an internal standard for pressure determination according to Ref. [34]. The isothermal compressibility used for LaB_6 was $(0.58 \pm 0.03) \times 10^{-11}$ Pa^{-1} [35]. The q range was calibrated using silver behenate (Rose Chemicals) [36]. All measurements were carried out at ~293 K.

IV. RESULTS AND DISCUSSION

We first recall the phase behavior of PF2/6 as observed in ambient (atmospheric) XRD. The crystalline (Hex) phase gives reflections arising from the lateral two-dimensional hexagonal packing of the chains and occurs at positions $q = 0.43$ Å^{-1} (100), 0.75 Å^{-1} (110), 0.86 Å^{-1} (200), etc., a series which decays rapidly in a paracrystalline fashion [23]. The order along the main chain is dominated by a reflection at $q = 0.78$ Å^{-1}. This corresponds to ~8 Å monomer repeat and (assuming 21/4 helix) is indexed as 00 21 [26,27]. In practice, 110 and 00 21 are the two most prominent reflections, but for the nonaligned samples they are difficult to tell apart at room temperature but are more easily separated following thermal expansion. At room temperature and ambient pressure the hexagonal cell parameter is $c = 16.7$ Å and the calculated density is ~0.99 g/cm^3.

At about 170 °C, HMW-PF2/6 undergoes a Hex-Nem transition, with its position depending on the molecular weight [23]. The Nem state shows slightly smaller monomer repeat (7.8 Å versus 8.1 Å) than the crystalline Hex state. This difference corresponds to a change in the torsional angle between adjacent repeat units from 65° (for 21/4 helix) to approximately 50°, i.e., closer to the minimum-energy conformation that is found at 43° [22]. The corresponding reflection (at $q = 0.8$ Å^{-1}) diminishes but stays relatively sharp. In contrast, the hexagonal reflections vanish totally leaving a single broad hump at $q = 0.71$ Å^{-1}, indicating 10.2 Å average distance between chains. The calculated density is ~0.92 g/cm^3.

Another Nem state is formed at low temperatures either in HMW-PF2/6 following rapid cooling or in LMW-PF2/6 ($M_n < M^*_{n0}$). In this case, the sharp 7.8 Å peak is still obtained, while the lateral order reduces to two broad peaks at 0.45 and 0.8 Å^{-1}. This state was originally described as "glassy nematic," so we shall also call it Nem phase (or LMW-Nem) although the term "weakly hexagonal crystalline" might also apply. In Ref. [23] it is shown how the broad peaks seamlessly transform into 100 and 110 reflections with a noticeable increase in the lattice parameter as the structure changes to Hex during heating. The distinction between LMW-Nem and HMW-Nem seems to be that the former preserves the "three-chain aggregate" of the Hex state. Assuming a weak hexagonal order, the calculated density for LMW-Nem is 1.12 g/cm^3, i.e., significantly higher than in the Hex phase.

Figure 2(a) plots WAXS curves of 29/68-PF2/6 at selected pressures showing the region around 00 21 reflection. Figure

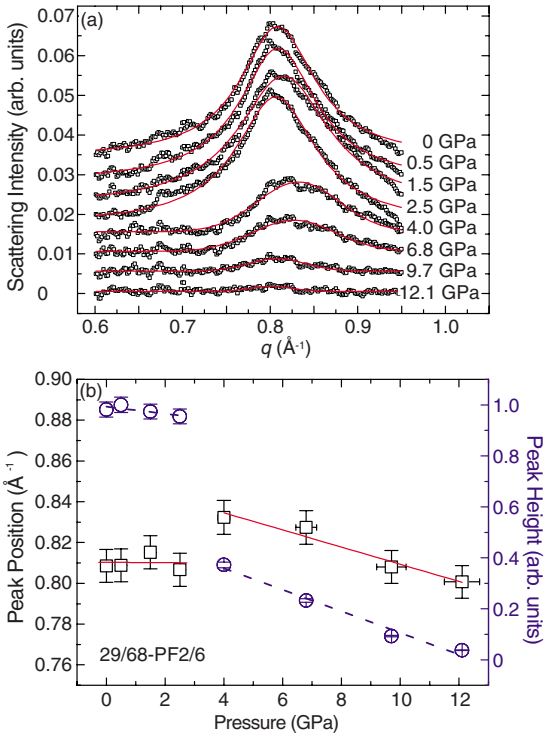

FIG. 2. (Color online) (a) X-ray scattering patterns of 29/68-PF2/6 with increasing pressure (from top to bottom). Solid red lines represent fits to the expected 00 21 reflection. (b) The position (black squares) and height (blue circles) of the expected 00 21 reflection of the same data. Linear fits (solid red and dashed blue lines) are a guide to the eye.

2(b) plots the peak height and position as functions of applied pressure. Both parameters remain essentially constant until 2–4 GPa where the intensity suddenly drops, followed by a slight peak shift toward higher scattering angles. When the pressure is raised from 4 GPa beyond 10 GPa, the intensity of 00 21 reflection tends to decrease still while the maximum moves back to the lower angles. Upon decreasing pressure, the peak retraces toward the original position but with a significant hysteresis (data not shown).

Mårdalen *et al.* [10] showed how the x-ray reflection 020 arising from the distance between POT chains shifts gradually and monotonically in one direction at elevated pressures. This is understood as a gradual planarization of the thiophene chains, while preserving the lamellar overall structure of the ambient pressure. By comparison, the data in Fig. 2 do not follow gradual but relatively abrupt changes in the peak height, and the peak position changes back and forth. This is reminiscent of a structural transition and may indicate that the hexagonal overall structure is transformed.

Figure 3 plots WAXS curves of 32/58-PF2/6 at selected pressures. The data quality is better than in Fig. 2, and besides meridional 00 21 reflection vestiges of equatorial 110, 100, and 101 reflections may be seen. It is also possible that 00 21 reflection contains remnants of 200 peak (cf. Fig. 7 in Ref. [23]). Relative peak areas for the considered 00 21 and putative 110 reflections are listed in Table I. Akin to the case of 29/68-PF2/6, the intensity of 00 21 peak remains constant up to 1.8 GPa but is significantly reduced when the pressure

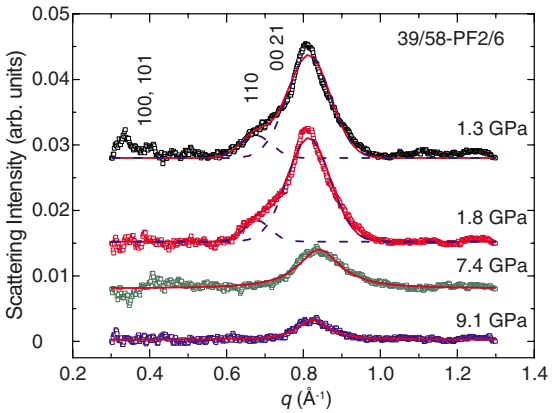

FIG. 3. (Color online) X-ray scattering patterns of 35/58-PF2/6 at selected pressures. From top to bottom: 1.3 GPa (black symbols), 1.8 GPa (red symbols), 7.4 GPa (green symbols), and 9.1 GPa (blue symbols). Dashed blue lines represent fits to the expected 110 and 00 21 reflections. Solid red lines represent the overall fit. Also shown are the positions of hexagonal reflections 100 and 101.

is increased from 1.8 to 7.4 GPa. A subtle peak shift toward higher scattering angles and back again is reproduced as well. The supposed 110 peak that is present up to 1.8 GPa but disappears with the diminished 00 21 peak. This observation is consistent with the idea of structural transition from the Hex phase. The peak position is lower than expected for ambient pressure. When discussing the interpretation of the supposed structural transition, we consider the possible planarization of the helical main chain and the interplay of Hex and (glassy) Nem structures.

It seems reasonable that the static pressure would tend to planarize twisted main chains since planar chains allow locally closer interchain contact. Assuming that PF2/6 has 21/4 helical backbone, in which the torsional angle is 65° (i.e., cis-type, meaning that side chains of adjacent monomers are on the same side), planarization causes more kink to the backbone. This would reduce monomer repeat and increase the 0.8 $Å^{-1}$ peak position, exactly as observed. The increased splay (curvature) along the chain may also stabilize the structure as neighboring chains would oppose the increase in average chain radius. Thus, the decrease in the monomer repeat stays modest. It is also possible that at the pressures above the seen transition (>6 GPa), a twist from cis to trans in the torsional angles may be necessary to reduce the chain diameter (for more efficient packing) and also to allow further planarization otherwise hindered by side-chain steric effects. In this case, the direction of peak shift

TABLE I. Peak position and integrated intensity for 39/68-PF2/6 at selected pressures; $T=293$ K.

Pressure (GPa)	Peak position ($Å^{-1}$)	Peak area	Peak position ($Å^{-1}$)	Peak area
1.3 ± 0.1	0.68 ± 0.01	0.16	0.81 ± 0.01	1.00
1.8 ± 0.1	0.68 ± 0.01	0.12	0.81 ± 0.01	1
7.4 ± 0.3			0.84 ± 0.01	0.56
9.1 ± 0.5			0.83 ± 0.01	0.21

should reverse toward smaller angles [cf. Fig. 2(b)]. Again, the changes are subtle as the theoretical upper limit of the monomer period for a completely trans backbone is only about 8.3 Å. A complete trans backbone is, of course, not possible due to the orthohydrogen in the main chain.

It is interesting that elsewhere, by studying oriented PF2/6 chains, King *et al.* [37] detailed how the phosphorescence emission of PF2/6 is dominated by a component perpendicular to the chain. If the polymer backbone adopted a more planar conformation at high pressure and if this sample was moreover macroscopically prealigned, the question of the planarization of helical main chain could be definitely answered.

The phase transition observed at 2–4 GPa resembles the high-temperature Hex-Nem transition. The weakening of 00 21 reflection and the disappearance of *hk*0 reflections indicate loss of crystallinity. This behavior, again, differs from the lamellar POT that shows a moderate increase in crystallinity with increasing pressure [10]. On the other hand, as shown for another poly(*p*-phenylene) (PPP)-type polymer elsewhere [38], the HMW-PF2/6 material should almost certainly occur in the glassy state. Thus, the considered Nem phase could be understood as a system with one-dimensional long-range order and not as an ordered fluid. In this phenomenological idea the degree of crystallinity changes with increasing pressure.

All parameters in Eq. (12) are either estimated in Ref. [23] ($f \approx 0.4$, $A=90$ K, and $M_{n0} \approx 10^4$ g/mol) or may be estimated independently (the densities). If we select $T_{ref} \approx 150\ ^\circ\mathrm{C}=423$ K as the transition temperature at atmospheric pressure, $P_{ref} \approx 0.1$ MPa, this yields

$$P^* \sim 10^3\ \mathrm{J}\frac{\rho_N \rho_H}{\rho_N - \rho_H}. \tag{13}$$

If the order of magnitude of densities was $\rho_i \sim 1$ g/cm^3 and their difference is $(\rho_N - \rho_H)/\rho_N \sim 0.1\%$, we would obtain $P^* \sim 1$ GPa. This would correspond to the order of magnitude of the experimentally observed 2–4 GPa. The exact density difference is difficult to measure, and therefore we cannot make a quantitative connection between theory and experiment. Our earlier estimates [23] were based on the assumption of hexagonal packing in the Nem state and are inaccurate even if this assumption was correct, because lattice parameters are not reliably determined for weakly ordered materials. The direction of the density change, however, predicts the Hex-Nem transition with increased pressure.

All theoretical considerations above are for nonglassy materials, while PF2/6 at elevated pressure is likely in the glassy state as indicated by the PPP analogy [38]. In alternative analogy PF2/6 may be understood as a specific block copolymer of rigid (backbone) and flexible (side-chain) blocks and Hex-Nem transition as an order-disorder transition. For the diblock copolymers the decrease in the free volume and the increase in the segregation effect usually mean that the thermal fluctuation effects decrease and the order-disorder temperature (T_{ODT}) increases with increasing pressure [39,40]. This depends on the polymer symmetry, so that T_{ODT} increases with increasing pressure only for nearly symmetric polymer but decreases with increasing pressure for the nonsymmetric case [41]. Even for the symmetric diblock copolymer, the transition depends on the side-chain length so that, for instance, for symmetric styrene/*n*-alkyl methacrylate block copolymers pressure suppresses mixing either for very short ($n=1$) or for very long ($n>1$) side chains of methacrylate [42]. The pressure-dependent phase transitions may also be understood in terms of Flory-type interaction parameters χ_{app} and χ_{comp} that represent unfavorable exchange energy and effects of compressibility difference between different blocks, respectively. As these contribute oppositely to the phase stability under compression, both increase and decrease in T_{ODT} are possible [43]. A phase transition may also occur in the glassy state as known for fluorene molecules at ~4 GPa [11].

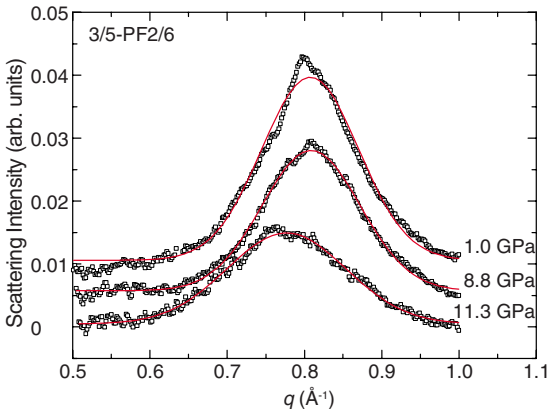

FIG. 4. (Color online) X-ray scattering patterns of 3/5-PF2/6 at selected pressures. Solid red lines represent fits to the expected 00 21 reflection.

We place finally attention on the LMW-PF2/6. As the molecular weight is below M^*_{n0}, the polymer is in the glassy Nem phase at ambient temperature and pressure. Figure 4 plots WAXS curves of 3/5-PF2/6 when the pressure is shifted from 1 to 11.3 GPa. The maximum at 0.8 Å^{-1} is present and shows a slight decrease and broadening with increasing pressure and, above 9 GPa, a shift toward lower scattering angles. In this case we do not observe a transition at 2–4 GPa, because Hex order is negligible in the first place. Above 9 GPa the behavior is, in principle, similar to 29/68-PF2/6.

V. CONCLUSIONS

Although qualitatively, we have conducted a WAXS experiment of PF2/6 at elevated pressures. The data show evidence for a morphological transition of HMW-PF2/6 with increasing pressure. This transition seems to occur at two stages. An initial planarization of 21-helical main chain occurs between 2 and 4 GPa and also suppresses intermolecular order. This is coupled with the transition from crystalline Hex to glassy Nem structure. The helical structure of the main chains is released further at higher pressures (7–9 GPa), resulting in a loss of registry between chains. Only the latter stage is proposed for LMW-PF2/6. This transition is phenomenologically consistent with the previously reported transition which is observed by high pressure PL and Raman

scattering experiments and which indicates a structural reorganization between 2 and 4 GPa. This tendency differs from the high pressure behavior of lamellar POT in which case the crystalline fraction increases with increasing pressure. Future research will be focusing on the background reduction and therefore on more accurate determination of structural parameters.

ACKNOWLEDGMENTS

M.K. and S.G. thank M. J. Winokur of the University of Wisconsin–Madison for discussions. M.K. received funding from the European Community's Seventh Framework Programme (FP7/2007–2013) under Grant Agreement No. 226716.

[1] A. Y. Grosberg and A. R. Khokhlov, *Statistical Physics of Macromolecules* (American Institute of Physics, Woodbury, NY, 1994).
[2] H. Menzel, in *Polymeric Materials Encyclopedia*, edited by J. C. Salamone (CRC Press, Boca Raton, FL, 1996), p. 2916.
[3] G. Wegner, Macromol. Chem. Phys. **204**, 347 (2003).
[4] M. J. Winokur, in *Handbook of Conducting Polymers*, edited by T. A. Skotheim and J. R. Reynolds (CRC Press LLC, Boca Raton, FL, 2007), Vol. 1, p. 1.
[5] R. Abbel, A. P. H. J. Schenning, and E. W. Meijer, J. Polym. Sci., Part A: Polym. Chem. **47**, 4215 (2009).
[6] D. Neher, Macromol. Rapid Commun. **22**, 1366 (2001).
[7] M. Knaapila and M. J. Winokur, Adv. Polym. Sci. **212**, 227 (2008).
[8] S.-A. Chen, H.-H. Lu, and C.-W. Huang, Adv. Polym. Sci. **212**, 49 (2008).
[9] A. Katrusiak, Acta Crystallogr., Sect. A: Found. Crystallogr. **64**, 135 (2008).
[10] J. Mårdalen, Y. Cerenius, and P. Häggkvist, J. Phys.: Condens. Matter **7**, 3501 (1995).
[11] G. Heimel, K. Hummer, C. Ambrosch-Draxl, W. Chunwachirasiri, M. J. Winokur, M. Hanfland, M. Oehzelt, A. Aichholzer, and R. Resel, Phys. Rev. B **73**, 024109 (2006).
[12] V. Morandi, M. Galli, F. Marabelli, and D. Comoretto, Phys. Rev. B **79**, 045202 (2009).
[13] M. Chandrasekhar, S. Guha, and W. Graupner, Adv. Mater. **13**, 613 (2001).
[14] S. Guha, W. Graupner, R. Resel, M. Chandrasekhar, H. R. Chandrasekhar, R. Glaser, and G. Leising, J. Phys. Chem. A **105**, 6203 (2001).
[15] M. Hangyo, K. Itakura, S. Nakashima, A. Mitsuishi, H. Matsuda, H. Nakanishi, M. Kato, and T. Kurata, Solid State Commun. **60**, 739 (1986).
[16] K. Paudel, M. Arif, M. Chandrasekhar, and S. Guha, Phys. Status Solidi B **246**, 563 (2009).
[17] K. Paudel, H. Knoll, M. Chandrasekhar, and S. Guha, J. Phys. Chem. A **114**, 4680 (2010).
[18] J. P. Schmidtke, R. H. Friend, and C. Silva, Phys. Rev. Lett. **100**, 157401 (2008).
[19] J. P. Schmidtke, J.-S. Kim, J. Gierschner, C. Silva, and R. H. Friend, Phys. Rev. Lett. **99**, 167401 (2007).
[20] M. Knaapila, B. P. Lyons, K. Kisko, J. P. Foreman, U. Vainio, M. Mihaylova, O. H. Seeck, L.-O. Pålsson, R. Serimaa, M. Torkkeli, and A. P. Monkman, J. Phys. Chem. B **107**, 12425 (2003).
[21] G. Lieser, M. Oda, T. Miteva, A. Meisel, H.-G. Nothofer, U. Scherf, and D. Neher, Macromolecules **33**, 4490 (2000).
[22] B. Tanto, S. Guha, C. M. Martin, U. Scherf, and M. J. Winokur, Macromolecules **37**, 9438 (2004).
[23] M. Knaapila, R. Stepanyan, M. Torkkeli, B. P. Lyons, T. P. Ikonen, L. Almásy, J. P. Foreman, R. Serimaa, R. Güntner, U. Scherf, and A. P. Monkman, Phys. Rev. E **71**, 041802 (2005).
[24] H.-Z. Tang, M. Fujiki, and T. Sato, Macromolecules **35**, 6439 (2002).
[25] L. Wu, T. Sato, H.-Z. Tang, and M. Fujiki, Macromolecules **37**, 6183 (2004).
[26] M. Brinkmann, N. Charoenthai, R. Traiphol, P. Piyakulawat, J. Wlosnewski, and U. Asawapirom, Macromolecules **42**, 8298 (2009).
[27] M. Knaapila, M. Torkkeli, and A. P. Monkman, Macromolecules **40**, 3610 (2007).
[28] C. M. Martin, S. Guha, M. Chandrasekhar, H. R. Chandrasekhar, R. Guentner, P. Scanduicci de Freitas, and U. Scherf, Phys. Rev. B **68**, 115203 (2003).
[29] S. Guha and M. Chandrasekhar, Phys. Status Solidi B **241**, 3318 (2004).
[30] L. D. Landau and E. M. Lifshitz, *Statistical Physics* (Pergamon, Oxford, 1980).
[31] M. Grell, W. Knoll, D. Lupo, A. Meisel, T. Miteva, D. Neher, H.-G. Nothofer, U. Scherf, and A. Yasuda, Adv. Mater. **11**, 671 (1999).
[32] Y. Cerenius, K. Ståhl, L. A. Svensson, T. Ursby, Å. Oskarsson, J. Albertsson, and A. Liljas, J. Synchrotron Radiat. **7**, 203 (2000).
[33] C. Hansson, S. Carlson, D. Giveen, M. Johansson, S. Yong, and Å. Oskarsson, Acta Crystallogr., Sect. B: Struct. Sci. **62**, 474 (2006).
[34] P. Teredesai, D. V. S. Muthu, N. Chandrabhas, S. Meenakshi, V. Vijayakumar, P. Modak, R. S. Rao, B. K. Godwal, S. K. Sikka, and A. K. Sood, Solid State Commun. **129**, 791 (2004).
[35] T. Lundström, B. Lönnberg, B. Törmä, J. Etourneau, and J. M. Tarascon, Phys. Scr. **26**, 414 (1982).
[36] W. Paszkowicz, P. Piszora, Y. Cerenius, S. Carlson, R. Minikayev, and E. Werner-Malento, Radiat. Phys. Chem. **78**, S105 (2009).
[37] S. M. King, H. L. Vaughan, and A. P. Monkman, Chem. Phys. Lett. **440**, 268 (2007).
[38] A. Gitsas, G. Floudas, and G. Wegner, Phys. Rev. E **69**, 041802 (2004).
[39] D. A. Hajduk, S. M. Gruner, S. Erramilli, R. A. Register, and L. J. Fetters, Macromolecules **29**, 1473 (1996).
[40] M. Miyazawa, M. Takenaka, T. Miyajima, and T. Hashimoto, J. Appl. Crystallogr. **36**, 656 (2003).
[41] H. Xu, H. Liu, and Y. Hu, Macromol. Theory Simul. **16**, 262 (2007).
[42] A.-V. G. Ruzette, A. M. Mayes, M. Pollard, T. P. Russell, and B. Hammouda, Macromolecules **36**, 3351 (2003).
[43] J. Cho, Macromolecules **35**, 5697 (2002).